Received: 28 August 2020 | Revised: 16 December 2020 | Accepted: 28 December 2020

DOI: 10.1096/fj.202002022R

RESEARCH ARTICLE

THE FASEB JOURNAL

Bifunctional protein PCBD2 operates as a co-factor for hepatocyte nuclear factor 1β and modulates gene transcription

Lotte E. Tholen[1] | **Caro Bos**[1] | **Pascal W. T. C. Jansen**[2] | **Hanka Venselaar**[3] | **Michiel Vermeulen**[2] | **Joost G. J. Hoenderop**[1] | **Jeroen H. F. de Baaij**[1]

[1]Department of Physiology, Radboud Institute for Molecular Life Sciences, Radboud University Medical Center, Nijmegen, The Netherlands

[2]Department of Molecular Biology, Faculty of Science, Radboud Institute for Molecular Life Sciences, Oncode Institute, Radboud University Nijmegen, Nijmegen, The Netherlands

[3]Centre for Molecular and Biomolecular Informatics, Radboud Institute for Molecular Life Sciences, Radboud University Medical Center, Nijmegen, The Netherlands

Correspondence
Jeroen H. F. de Baaij, Department of Physiology, Radboud Institute for Molecular Life Sciences, Radboud university medical center, P.O. Box 9101, 6500 HB, Nijmegen, The Netherlands.
Email: jeroen.debaaij@radboudumc.nl

Funding information
Nierstichting (Dutch Kidney Foundation), Grant/Award Number: 17OKG07; Nederlandse Organisatie voor Wetenschappelijk Onderzoek (NWO), Grant/Award Number: Veni 016.186.012 and Vici 016.130.668; KWF Kankerbestrijding (Dutch Cancer Society)

Abstract

Hepatocyte nuclear factor 1β (HNF1β) is an essential transcription factor in development of the kidney, liver, and pancreas. HNF1β-mediated transcription of target genes is dependent on the cell type and the development stage. Nevertheless, the regulation of HNF1β function by enhancers and co-factors that allow this cell-specific transcription is largely unknown. To map the HNF1β interactome we performed mass spectrometry in a mouse kidney inner medullary collecting duct cell line. Pterin-4a-carbinolamine dehydratase 2 (PCBD2) was identified as a novel interaction partner of HNF1β. PCBD2 and its close homolog PCBD1 shuttle between the cytoplasm and nucleus to exert their enzymatic and transcriptional activities. Although both PCBD proteins share high sequence identity (48% and 88% in HNF1 recognition helix), their tissue expression patterns are unique. PCBD1 is most abundant in kidney and liver while PCBD2 is also abundant in lung, spleen, and adipose tissue. Using immunolocalization studies and biochemical analysis we show that in presence of HNF1β the nuclear localization of PCBD1 and PCBD2 increases significantly. Promoter luciferase assays demonstrate that co-factors PCBD1 and PCBD2 differentially regulate the ability of HNF1β to activate the promoters of transcriptional targets important in renal electrolyte homeostasis. Deleting the N-terminal sequence of PCBD2, not found in PCBD1, diminished the differential effects of the co-factors on HNF1β activity. All together these results indicate that PCBD1 and PCBD2 can exert different effects on HNF1β-mediated transcription. Future studies should confirm whether these unique co-factor activities also apply to HNF1β-target genes involved in additional processes besides ion transport in the kidney.

KEYWORDS

hepatocyte nuclear factor 1β, pterin-4a-carbinolamine dehydratase 2, transcription co-factor

Abbreviations: ADTKD-HNF1β, autosomal dominant tubulointerstitial kidney disease subtype HNF1β; BH4, tetrahydrobiopterin; CBP, CREB-binding protein; CE, cellular extract; CD, collecting duct; DCT, distal convoluted tubule; FDR, false discovery rate; HAT, histone acetyltransferase; HDAC1, histone deacetylase 1; HNF1α, hepatocyte nuclear factor 1α; HNF1β, hepatocyte nuclear factor 1β; iBAQ, intensity-based absolute quantification; mIMCD3, mouse inner medullary collecting duct 3; NE, nuclear extract; NPE, nuclear pellet extract; PAH, phenylalanine hydroxylase; PT, proximal tubule; PCBD, pterin-4 alpha-carbinolamine dehydratase; TAL, thick ascending loop of Henle.

1 | INTRODUCTION

Hepatocyte nuclear factor 1β (HNF1β) is an essential transcription factor for development and function of the kidney, liver, pancreas, and genital tract.[1] Mutations or deletion in HNF1β cause autosomal dominant tubulointerstitial kidney disease subtype HNF1β (ADTKD-HNF1β), which is characterized by renal malformations and cysts (80%), hypomagnesemia (50%), maturity-onset diabetes of the young (MODY5) (40%), and genital tract malformations.[2,3] Although the transcriptional targets are still being discovered, HNF1β-regulated genes related to cyst development and ion transport in the kidney include *PKHD1, PKD2, FXYD2, KCNJ16, and TMEM27*.[4-7]

HNF1β exerts its function in homo- or heterodimeric complexes with HNF1α and its activity is partially regulated by binding to co-factors. In the past decades several HNF1β co-factors have been identified including p300/CBP-associated factor (P/CAF), CREB-binding protein (CBP), two histone acetyltransferases (HAT), and histone deacetylase 1 (HDAC1).[8,9] Moreover, the dimerization domain of HNF1β interacts with co-factor Pterin-4a-carbinolamine dehydratase 1 (PCBD1) and forms heterotetramers in a 2:2 fashion.[10] PCBD1 is part of an interesting group of multifunctional proteins called moonlighting proteins that fulfill multiple autonomous functions without attributing these roles to different protein domains.[11] Next to its co-factor function, PCBD1 is localized in the cytosol where it forms homotetramers and regenerates tetrahydrobiopterin (BH4) together with dihydropteridine reductase.[10,12] BH4 functions as a co-factor for phenylalanine hydroxylase (PAH) and other aromatic amino acid hydrolases.[13] Interestingly, mutations in PCBD1 cause magnesium ($Mg2^{+}$) wasting and diabetes, phenotypes also observed in patients with HNF1β mutations.[14,15] Mg^{2+} wasting in these patients might be explained by the ability of PCBD1 to enhance HNF1β-mediated promoter activation of *FXYD2*, which is involved in Mg^{2+} reabsorption in the distal convoluted tubule (DCT).[3,15]

HNF1β controls the gene expression in epithelial cells of many organs, regulating a different set of target genes in every tissue.[1] Moreover, in kidney development, HNF1β plays a recurring role during various stages regulating branching morphogenesis, collecting duct (CD) differentiation, and tubular epithelial organization.[16,17] This tissue- and time-specific gene regulation of HNF1β might be explained by differential binding to and expression of co-factors.

In the current study, we aim to identify new interaction partners of HNF1β and to study their role in regulating HNF1β function. Mass spectrometry analysis of a mouse kidney cell line reveals PCBD2, a homolog of PCBD1, as a novel binding partner of HNF1β. Furthermore, the differential effects of the two dimerization factors on HNF1β-mediated gene transcription of genes involved in renal electrolyte handling are uncovered.

2 | MATERIALS AND METHODS

2.1 | Cell culture

Mouse inner medullary collecting duct (mIMCD3) Flp-in cells were grown in DMEM/F-12 1:1 (Sigma-Aldrich, St. Louis, MO, USA) containing 10% FCS (v/v) (Biowest, Kansas City, MO, USA) and 1% (w/v) sodium pyruvate at 37°C in a humidity-controlled incubator with 5% (v/v) CO_2. Human Embryonic Kidney (HEK293) cells were grown in DMEM (Lonza, Basel, Switzerland) containing 10% (v/v) FCS, 0.1 mM nonessential amino acids, and 2 mM L-glutamine at 37°C in a humidity-controlled incubator with 5% (v/v) CO_2.

2.2 | DNA constructs

Human *PCBD2* full length cDNA was amplified from a pDNR-LIB (clone IRAUp969E0391D, Source BioSciences, Nottingham, UK) using PCR and subcloned into a pCI-Neo IRES mCherry expression vector. Human *HNF1β* full length cDNA was amplified from *HNF1β* pCMV-SPORT6 (clone IRATp970A0421D, Source BioSciences) using PCR and subcloned into the pCDNA5_frt expression vector and myc-tagged at the NH_2 terminal.[5] Human HA-*HNF1β* pCINEO, Flag-*PCBD1* pCINeo, *KCNJ16* promoter pGL3, and *FXYD2* pGL3 vectors were generated previously.[4,5,15] Mutant *PCBD1*-T51S, *PCBD2*-S78T, and *PCBD2* lacking the amino (N)-terminus (AA 1-27) constructs were generated using the Q5 site-directed mutagenesis according to the manufacturer's protocol (New England Biolabs, Ipswich, US).

2.3 | Generation of stable cell line

mIMCD3 Flp-in positive cells were preselected with 100 μg/mL zeocin (Thermo Fisher Scientific, Waltham, MA, USA) before transfection. Cells were seeded in 6-well plates and stably transfected with 1.5 μg pCDNA5_frt Myc-*HNF1β* or empty pCDNA5_frt and 1.5 μg pOG44 constructs using lipofectamine 3000 (Thermo Fisher Scientific) at a 1:3 DNA to lipofectamine ratio. Two days after transfection positive cells were selected with 600 μg/mL of hygromycin (Thermo Fisher Scientific). Positive colonies appeared after 2 weeks and were isolated and grown until confluency. Cells were maintained in presence of 400 μg/mL of hygromycin.

2.4 | Nuclear and cytoplasmic extract isolation

Nuclear extracts from mIMCD3 Flp-in myc-HNF1β, mIMCD3 Flp-in WT, or HEK293 cells were generated as described previously.[18] In short, cells were washed twice with PBS before harvesting. Subsequently, cells were incubated in hypotonic buffer (10 mM KCl, 1.5 mM $MgCl_2$, and 10 mM Hepes-KOH pH 7.9) containing 0.15% (v/v) NP-40 (Roche, Basel, Switzerland) and protease inhibitors and homogenized using a type B pestle (tight). Homogenized cells were centrifuged for 15 minutes at 3200 *g* to pellet nuclei. Supernatant was collected to obtain cytoplasmic protein extract. Nuclei were incubated with lysis buffer (420 mM NaCl, 20% (v/v) glycerol, 2 mM $MgCl_2$, 0.2 mM EDTA, and 20 mM Hepes-KOH/pH 7.9) containing 0.1% (v/v) NP-40 and protease inhibitors for 1 hour at 4°C. Lysed nuclei were centrifugated for 30 minutes at 20 000 *g* at 4°C to obtain nuclear protein extracts.

To generate nuclear pellet extracts, remaining pellets were solubilized by resuspension in four volumes of RIPA buffer (150 mM NaCl, 50 mM Tris pH 8.0, 1% (v/v) NP-40, 5 mM $MgCl_2$, and 10% (v/v) glycerol). Benzonase (Merck Millipore, Burlington, Massachusetts, USA) was added at 1000 U per 100 µL nuclear pellet. Samples were incubated at 37°C while shaking until the pellet disappeared. The extracts were cleared by centrifugation at 18 000 *g* for 15 minutes at 4°C.

2.5 | Western blotting

Nuclear and cytoplasmic protein extracts from mIMCD3 Flp-in myc-HNF1β and mIMCD3 Flp-in wild-type (WT) cells were denatured in Laemmli sample buffer (2% (v/v) SDS, 0.01% (w/v) bromophenol blue, 6% (v/v) glycerol, and 60 mM Tris-HCl/pH 6.8) containing 100 mM of DTT for 30 minutes at 37°C. Subsequently, samples were subjected to SDS-PAGE and used for immunoblotting. Rabbitanti-c-Myc (9E10, 1:500, Santa Cruz Biotechnology, CA, USA), Rabbit anti-HNF1β (SC-22840, 1:500, Santa Cruz Biotechnology), mouse anti-HA (1:5,000, 6E2, Cell signaling) or mouse anti-Flag M2 (F1804, 1:5,000, Sigma-Aldrich) primary antibodies and peroxidase-conjugated sheep anti-mouse (A6782, 1:10,000; Sigma-Aldrich) and peroxidase-conjugated goat anti-rabbit (A4914, 1:10,000; Sigma-Aldrich) secondary antibodies were used to visualize proteins.

2.6 | Myc pull-down and sample preparation for Mass spectrometry

Nuclear extracts from mIMCD3 Flp-in myc-HNF1β and mIMCD3 Flp-in WT cells were subjected to Myc-affinity enrichment using Myc-Trap beads (ChromoTek, Planegg-Martinsried, Germany). Three pull-downs were performed for each sample. Each pull-down, consisting of 1 mg of nuclear extract or 800 µg of nuclear pellet extract, was incubated with beads in incubation buffer (300 mM NaCl, 0.1% (v/v) NP-40, and 0.5 mM DTT 20 mM HEPES-KOH/pH7.9) for 90 minutes on a rotating wheel at 4°C. Ethidium bromide was added to the pull-down reaction (10 mg/mL) to prevent indirect, DNA-mediated interactions. Subsequently, beads were washed two times with incubation buffer containing 0.5% (v/v) NP-40, two times with PBS containing 0.5% (v/v) NP-40, and lastly two times with only PBS. After washing, the supernatant was removed completely and precipitated proteins were subjected to on-bead trypsin digestion as described previously.[19] Beads were resuspended in 50 µL elution buffer (2 M Urea, 10 mM DTT, and 100 mM Tris-HCl/pH 8) and incubated on a shaker for 20 minutes at room temperature (RT) to partly denature the proteins. Subsequently, iodoacetamide (Sigma-Aldrich) was added to the beads to a final concentration of 50 mM and incubated in the dark for 10 minutes on a shaker at RT to alkylate cysteines. After alkylation, 0.25 mg of trypsin (Promega, Madison, WI, USA) was added to the beads for 2 hours, shaking at RT to digest proteins from the beads. The supernatant was collected. To collect all peptides from the beads, another 50 µL of elution buffer was added to the beads and incubated for 5 minutes at RT, supernatant was collected and combined with the first supernatant. To ensure complete digestion of the proteins, 0.1 mg of trypsin was added to the supernatant and incubated overnight at RT. Next morning, digestion was stopped by adding trifluoroacetic acid (TFA) 0.5% (v/v). Tryptic peptides were loaded on C18 Stage tips as described previously.[20] Briefly, C18 Stage tips were washed with 50 µL of MeOH followed by buffer B (80% Acetonitrile, 0.1% v/v TFA), and two times buffer A (0.1% v/v TFA). Samples were loaded on stage tips by spinning for 10 minutes at 2400 *g*. Finally, loaded stage tips were washed twice with buffer A.

2.7 | Mass spectrometry and data analysis

Peptides were analyzed on reverse phase Easy-nLC 1000 coupled on-line to a Thermo Q-Exactive hybrid mass spectrometer (Thermo Fisher Scientific) using a 120-minute gradient of buffer B (80% Acetonitrile, 0.1% v/vTFA). Dynamic exclusion was enabled for 30 seconds.

Raw data were analyzed using the MaxQuant software suit,[21] using the default settings, trypsin as protease and the Mus musculus database. Label-free quantification and intensity-based absolute quantification (iBAQ) were enabled. The resulting protein groups file was further processed using Perseus.[22] The data were filtered for potential contaminants and reverse hits. Then, triplicates were

assigned to the control or test group. Data were logarithmized and proteins were then filtered to contain at least three valid values in one of the groups, assuming that a specific interactor may not have been identified in the control pull-downs. Missing values were imputed using the default settings. Statistical outliers for the Myc pull-down of the mIMCD3 Flp-in myc-HNF1β compared to mIMCD3 Flp-in WT were then determined using a two-tailed *t* test. Multiple testing correction was applied using a permutation-based false discovery rate (FDR) method in Perseus. Stoichiometry calculations are essentially as described.[23] The average iBAQ value obtained in the control pull-downs was subtracted from the iBAQ values obtained in each of the specific pull-downs. These values were then divided by the values of the bait protein in that pull-down. The remaining values were averaged and standard deviations were calculated. Data were visualized using the program R.

2.8 | Co-immunoprecipitation

HEK293 cells were seeded on 145 mm petri dishes and co-transfected with 20 μg Flag-*PCBD1* or Flag-*PCBD2* constructs with 20 μg HA-*HNF1β* construct or an empty pCINeo IRES mCherry vector using lipofectamine 2000 (Thermo Fisher Scientific) at a 1:1 DNA to lipofectamine ratio. Cells were harvested 48 hours after transfection and nuclear extracts were prepared as described above. The next incubation steps were all preformed under rotary agitation. A total of 25 μL A/G of PLUS-Agarose beads (Santa Cruz Biotechnology) were previously incubated overnight at 4°C with 1 μL of mouse anti-HA antibody (6E2, Cell Signaling Technology, Danvers, MA, USA). Beads were washed one time with PBS to remove the unbound antibodies. To bind antibodies covalently to the beads, beads were washed three times with 0.1 M of sodium borate-HCl/pH 9.3 and incubated for 30 minutes with 0.1 M of sodium borate containing 20 mM of DMP at RT. Subsequently, fresh 0.1 M of sodium borate containing 20 mM dimethyl pimelimidate (DMP, Sigma-Aldrich) was added and incubated for 15 minutes at RT. After incubation beads were washed four times with 50 mM of glycine-HCl/pH 2.5 and once with 0.2 M of Tris-HCl/pH 8.0. Beads were neutralized in 0.2 M of Tris-HCl/pH 8.0 for 2 hours at RT. After incubation Tris-HCl was removed and beads were resuspended in PBS to make a 1:1 slurry. After sampling the input control, equal amounts of protein of the remaining samples were incubated with the antibody beads overnight at 4°C. Next day beads were washed twice with incubation buffer (0.1% (v/v) NP-40) and twice with PBS. Samples were incubated for 30 minutes at 37°C in Laemmli sample buffer supplemented with 100 mM of DTT to separate the proteins from the beads. Proteins were detected by immunoblotting using mouse anti-HA (1:5000, 6E2, Cell signaling) or mouse anti-Flag M2 (F1804, 1:5000, Sigma-Aldrich) primary antibodies and peroxidase-conjugated sheep anti-mouse secondary antibodies (A6782, 1:10 000; Sigma-Aldrich).

2.9 | Immunocytochemistry

HEK293 cells were seeded in 12-well plates on fibronectin-coated glass coverslips and co-transfected with 666 ng HA-*HNF1β* or empty constructs with 333 ng Flag-*PCBD1* or Flag-*PCBD2* or empty constructs using lipofectamine 2000 (Thermo Fisher Scientific) at a 1:2 DNA to lipofectamine ratio. After 48 hours, cells were fixated with 4% (v/v) paraformaldehyde for 10 minutes followed by permeabilization for 10 minutes with 0.3% (v/v) Triton X-100 in PBS and finally incubated in blocking buffer for 30 minutes (16% (v/v) goat serum and 0.3% (v/v) Triton X-100 in PBS). Subsequently, fixed cells were incubated overnight at 4°C with a rabbit anti-Flag M2 antibody (F7425, 1:100, Sigma-Aldrich) and/or a mouse anti-HA antibody (1:100, 6E2, Cell signaling) diluted in blocking buffer. Next day cells were washed three times with PBS and incubated with secondary antibodies goat anti-rabbit antibody coupled to Alexa Fluor 647 (A32733, 1:300, Thermo Fisher Scientific) or goat anti-mouse coupled to Alexa Fluor 594 (A11005, 1:300, Thermo Fisher Scientific) or 488 (A-11029, 1:300, Thermo Fisher Scientific) together with 0.1 μg/mL of DAPI (D1306, Thermo Fisher Scientific) for 45 minutes at RT. Cells were washed three times with PBS and mounted with Fluoromount-G (Southern Biotech, Birmingham, AL, USA). Images were taken with a Zeiss LSM880 confocal microscope (Zeiss, Sliedrecht, The Netherlands) at 63x magnification. Images were analyzed using the software ImageJ.

2.10 | Immunohistochemistry

Stainings were performed on 3 μm sections of formalin-fixed, paraffin-embedded healthy human kidney tissue. For all staining protocols, paraffin sections were deparaffinized and rehydrated. Subsequently, sections were heat-treated with sodium-citrate-HCl/pH 6.0 and washed three times in 0.15 M of NaCl and 0.1 M of Tris-HCl/pH 7.6 (TN-buffer). Sections were permeabilized in TN-buffer containing 0.1% (v/v) Triton for 15 minutes. Endogenous peroxidase activity was blocked with 0.3% (v/v) H_2O_2 and unspecific binding sites were blocked with blocking buffers (Avidin/Biotin Blocking kit, BioLegend, San Diego, CA, USA). The sections were incubated with primary antibodies rabbit anti-PCBD2 (1:50, 200622-T08, Sino Biological, Vienna, Austria) overnight at 4°C. PCBD2 staining was enhanced

TABLE 1 Primer sequences

Gene name	Forward primer	Reversed primer
mHnf1b	5′-CATTGCACAGAGCCTCAACACC-3′	5′-GTTGAGAGAACTGGACGGGCTG-3′
mHnf1a	5′-ATGACACGGATGACGATGGG-3′	5′-GCCATGGGTCCTCCTGAAG-3′
mPcbd1	5′-TGGACATGGCCGGCAAGGC-3′	5′-CCCACAGCCCTCAGGTTTG-3′
mPcbd2	5′-CAATCAGGCGTTTGGCTTTATG-3′	5′-CCACAGTCATGCGAGGTG-3′
mGapdh	5′-TAACATCAAATGGGGTGAGG-3′	5′-GGTTCACACCCATCACAAAC-3′

using TSA fluorescence System (PerkinElmer). In order to co-stain PCBD2 with nephron markers, sections were incubated with the following primary antibodies for 4 hours at RT: guinea pig anti-AQP2 (1:200, home-made), sheep anti-UMOD (1:200, 8595-0054, Bio-Rad AbD Serotec, Hercules, CA, USA), and sheep anti-NCC (1:200). Human sections were incubated with Alexa Fluor 594 secondary antibodies (Thermo Fisher Scientific). Finally, sections were washed, incubated for 5 minutes with 0.1 μg/mL of DAPI (D1306, Thermo Fisher Scientific) and mounted with Fluoromount-G (Southern Biotech). Images were taken with an AxioCam MRm camera (Zeiss, Sliedrecht, The Netherlands) at 40x magnification. Zeiss Zen 2012 (Zeiss) software was used to acquire the images.

2.11 | Luciferase reporter assay

HEK293 cells were seeded in 24-well plates and transfected with 350 ng of the promoter firefly luciferase constructs (pGL3) previously generated containing the promoter of *FXYD2, KCNJ16,* or no promoter.[4,5] All three constructs were co-transfected with 25 ng of pCINEO-empty or pCINEO-h*HNF1B* combined with pCINEO-empty, pCINEO-*PCBD1*, pCINEO-*PCBD2*, pCINEO-*PCBD1*-T51S, pCINEO-*PCBD2*-S78T, or pCINEO-*PCBD2*-Δ1-27 constructs. Additionally, for controlling the transfection efficiency in each reaction, 10 ng of Renilla luciferase construct (pRL) under a CMV promoter was co-transfected and used to normalize luciferase counts in all conditions. Co-transfections were performed using polyethylenimine cationic polymer (PEI) (Thermo Fisher Scientific) in 1:6 DNA to PEI ratio. Firefly and Renilla luciferase luminescence were measured 48 hours after transfection with the dual-luciferase reporter assay (Promega) using a plate reader (VICTOR, PerkinElmer).

2.12 | Homology modeling of HNF1β interaction domain

No 3D-structure of the interaction domain of HNF1β is known. Therefore, we decided to build a homology model of residue 3-30 of HNF1β using PDB file 1F93 as template.[5] The fast YASARA[24] and WHAT IF[25] modeling script was used to create this model. This short stretch of residues shows 67% sequence identity. The model was superposed on PDB file 1F93 and 4C45 (not yet published) to obtain the final PCBD1/2—HNF1β complex.

2.13 | Real-time quantitative PCR

Tissues from C57BL/6N mice were isolated and total RNA was extracted from the tissues using TRIzol reagent (Thermo Fisher Scientific) according to the manufacturer's protocol.[26] The isolated RNA was subjected to DNase treatment (Promega). Subsequently, RNA was used for reversed transcription using the M-MLV protocol described by the manufacturer (Thermo Fisher Scientific). Obtained cDNA was used to determine gene expression levels by SYBR Green (Bio-Rad) real-time PCR using the CF96 real-time PCR detection system (Bio-Rad) and primers are listed in Table 1. mRNA levels were normalized for glyceraldehyde 3-phosphate dehydrogenase (*Gapdh*) expression.

2.14 | Statistical analysis (non-mass spectrometry experiments)

Data are expressed as means ± SD of at least three independent experiments. Differences were identified using Students *t* tests or two-way analysis of variance with correction for multiple testing using the Holm-Sidak procedure. $P < .05$ was considered to be statistically significant.

3 | RESULTS

3.1 | Co-factor PCBD2 interacts with HNF1β in the nucleus

To identify the co-factors that regulate HNF1β function, mass spectrometry analysis was performed in kidney cells to identify the interaction partners of HNF1β. Therefore, a mouse inner medullary collecting duct (mIMCD3) Flp-in cell line stably expressing Myc-HNF1β was generated (Figure S1A,B). Affinity purifications of Myc-HNF1β on

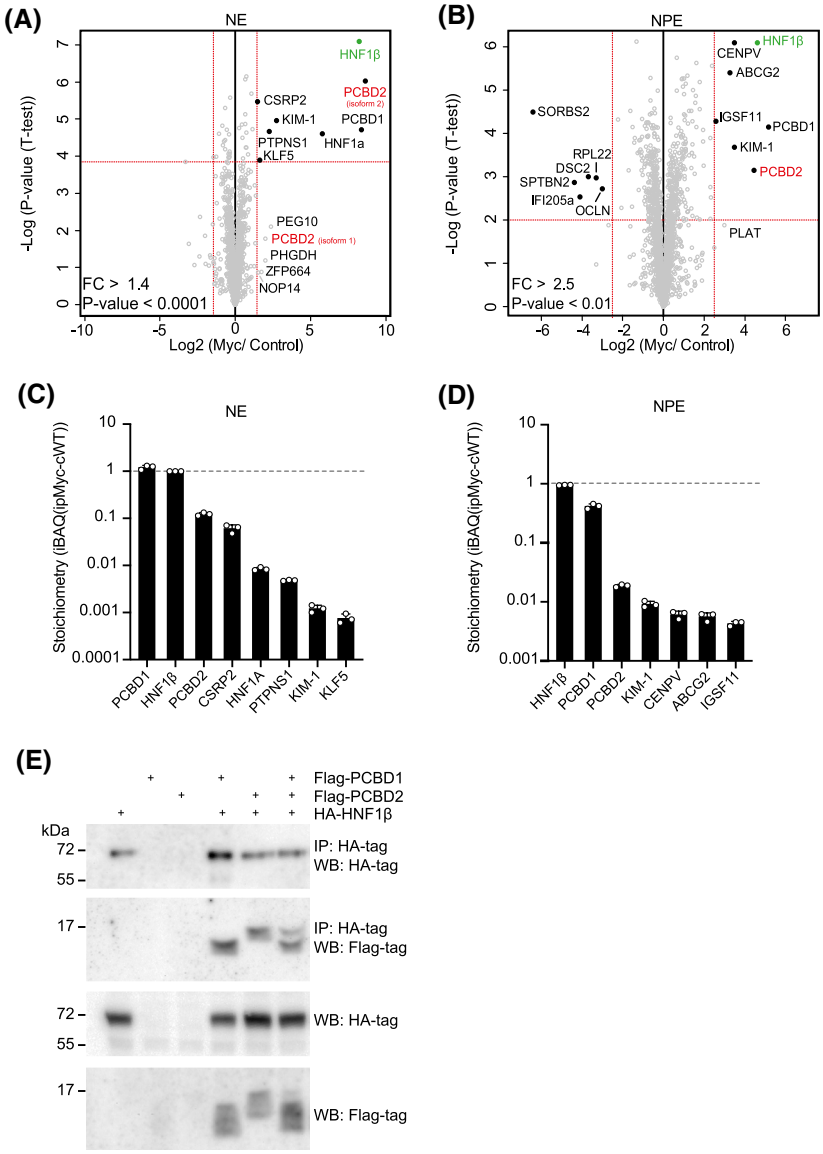

FIGURE 1 Co-factor PCBD2 interacts with transcription factor HNF1β. A,B, Nuclear extracts (NE) and nuclear pellet extracts (NPE) from mIMCD3 Flp-in Myc-HNF1β transgenic cell lines and mIMCD3 Flp-in WT cells are subjected to single-step Myc-affinity enrichment using Myc-Trap beads in triplicate. Statistically enriched proteins in the Myc pull-down are identified by permutation-based FDR-corrected *t* test. The intensity of the proteins in the Myc pull-down over the control is plotted against the −log10 *P* value and the red line indicates the permutation-based FDR threshold (thresholds NE: *P* value <.0001 and log2(FC) > 1.4 and thresholds NPE: *P* value <.01 and log2(FC) > 2.5). C,D, Stoichiometry calculations of the statistically significant interactors of Myc-HNF1β. Stoichiometry of the interactors is determined by calculating the abundance of the interactors in the specific pull-down (iBAQ value). The iBAQ values obtained in the control samples (WT mIMCD3 Flp-in cells) are subtracted from the iBAQ intensity in the Myc pull-down. The remaining values were scaled according to the abundance of Myc-HNF1β, resulting in the stoichiometry of the interactors relative to the bait. E, Flag-tagged PCBD1 or PCBD2 or mock DNA were transiently expressed in HEK293 cells with HA-tagged HNF1β. Immunoprecipitations on nuclear extracts using an anti-HA antibody were analyzed by Western blots using anti-HA and anti-Flag antibodies

nuclear extracts (NE) resulted in the identification of seven significant interactors, including PCBD2 (Figure 1A). Two known, previously identified interaction partners; HNF1α and PCBD1 were present among the proteins, validating our experimental setup (Figure 1A).[10,27] DNA pellets remaining after nuclear protein extraction were digested with nucleases to enable the extraction of proteins that bind to the DNA with high affinity. Similar to the NE, in the nuclear pellet extracts (NPE), we identified six interacting proteins, including PCBD1 and PCBD2, but not HNF1α (Figure 1B). PCBD1 showed a stoichiometry relative to HNF1β of 1 and 0.42 in the NE and NPE samples, respectively (Figure 1C,D). A stoichiometry of approximately 0.01 was calculated for HNF1α, suggesting that in 1% of the complexes HNF1β forms heterodimers with HNF1α. Furthermore, PCBD2 demonstrated a stoichiometry of 0.12

and 0.02 relative to HNF1β in the NE and NPE, respectively. The HNF1β-PCBD2 interaction was validated by coimmunoprecipitation assays in HEK293 cells transfected with constructs for HNF1β and PCBD2 using PCBD1 as control (Figure 1E).

3.2 | PCBD1 and PCBD2 translocate to the nucleus in presence of HNF1β

In the cytoplasm, PCBD1 and PCBD2 facilitate an enzymatic function in tetrahydrobiopterin recycling.[12,28] However, in the nucleus the proteins act as co-factors for HNF1α and HNF1β transcriptional activity. To study the cellular localization of PCBD1 and PCBD2, nuclear and cytoplasmic extracts were prepared of HEK293 cells transfected with *PCBD1* or *PCBD2* together with a mock or *HNF1β* construct and analyzed by Western blot analysis. As expected, HNF1β was exclusively present in the nuclear extracts (Figure 2A). In absence of HNF1β, PCBD1 and PCBD2 were predominantly present in the cytoplasmic extracts (Figure 2A). Conversely, quantification of the Western blots showed a 55% and 41% increase in nuclear localization of PCBD1 and PCBD2, respectively, as result of co-transfection with HNF1β (Figure 2B). Moreover, localization studies using immunocytochemistry in HEK293 cells demonstrated expression of PCBD2 in the nucleus and cytosol (Figure 2C). Co-transfection of PCBD2 and HNF1β increased nuclear localization of PCBD2 compared to cells only expressing PCBD2 (Figure 2D). Similar results were observed for PCBD1 (Figure 2C,D).

3.3 | PCBD2 and its close homolog PCBD1 display unique tissue expression patterns

The expression of *Pcbd1* and *Pcbd2* was examined in a mouse tissue panel by RT-qPCR to study tissue expression patterns of these highly related proteins. *Pcbd1* mRNA was predominantly expressed in kidney and liver while *Pcbd2* was also robustly expressed in lung, spleen, and fat tissue (Figure 3A). Additionally, mRNA levels of transcription factor *Hnf1b* and *Hnf1a* were measured in the mouse tissue panel. *Hnf1b* is primarily expressed in kidney, lung, and colon while *Hnf1a* is expressed in kidney, liver, and small intestines (Figure 3B).

HNF1β is expressed along the whole nephron and is important for kidney function.[1] To evaluate the localization

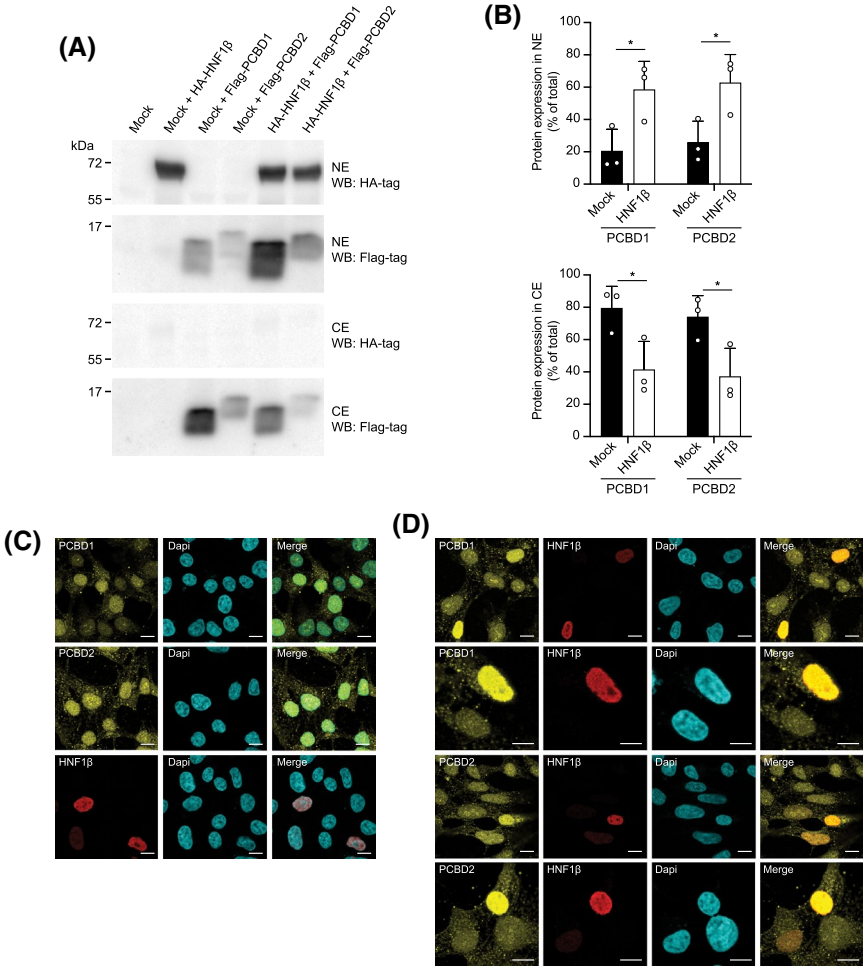

FIGURE 2 Co-factor PCBD1 and PCBD2 translocate to the nucleus in presence of HNF1β. A, Flag-tagged PCBD1 or PCBD2 or mock DNA was transiently expressed in HEK293 cells together with HA-tagged HNF1β. Nuclear extracts (NE) and cytoplasmic extracts (CE) were prepared and analyzed by Western blots (WB) using anti-HA and anti-Flag antibodies. B, Quantification of Western blots using FIJI image processing. Black bars represent data of PCBDs co-transfected with mock DNA and white bars represent PCBDs co-transfected with HNF1β. Data represents three independent experiments ± SD. * $P < .05$. C, Immunocytochemistry analysis of HEK293 transfected with HA-*HNF1β* or Flag-*PCBD1* or Flag-*PCBD2* constructs. Scale bar represents 10 μm. D, Immunocytochemistry analysis of HEK293 co-transfected with HA-HNF1β and Flag-PCBD1 or Flag-PCBD2 in a 2:1 ratio. Scale bar represents 10 μm.

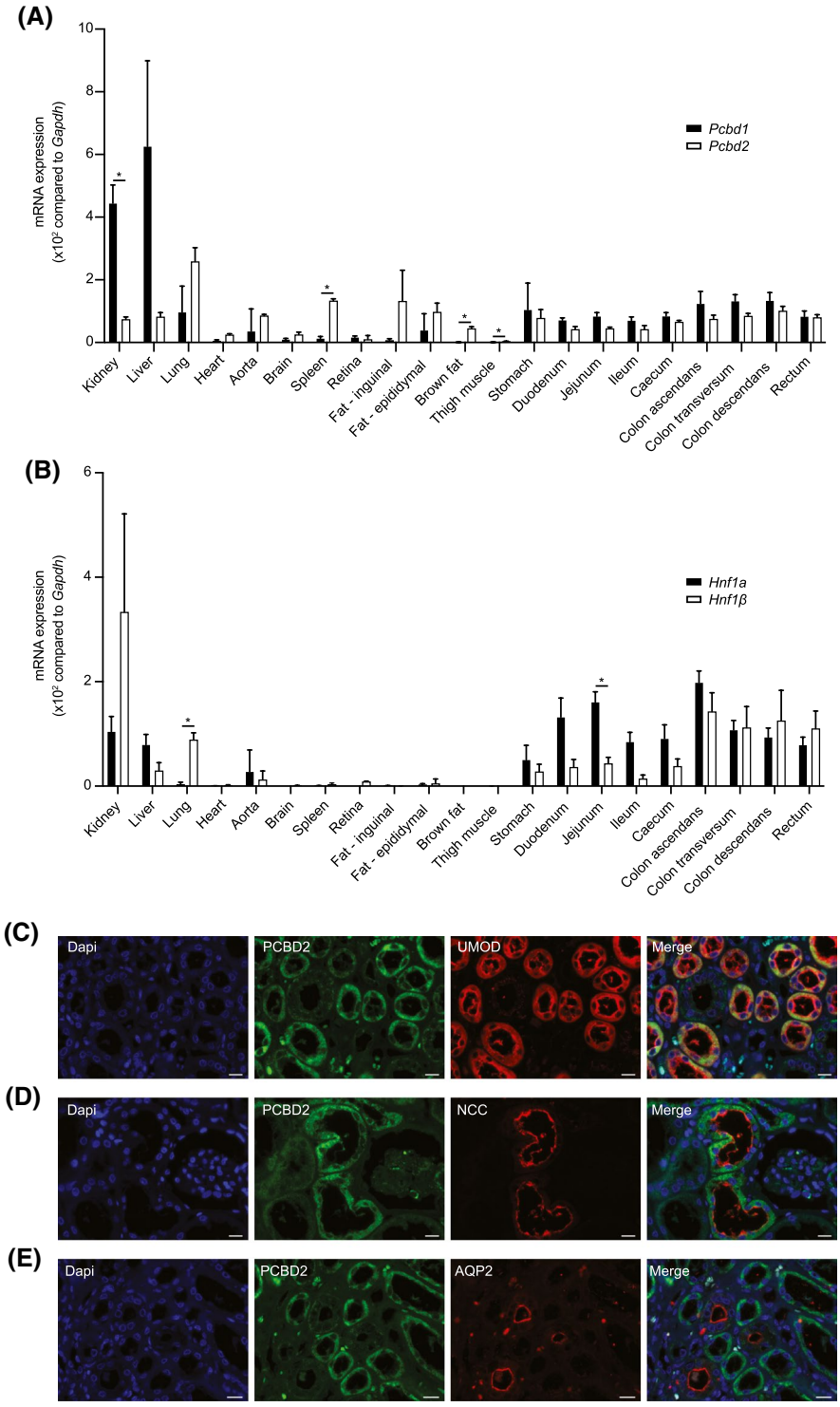

FIGURE 3 PCBD2 and PCBD1 display unique tissue expression patterns. A, *Pcbd1* (black bars) and *Pcbd2* (white bars) mRNA levels were measured in a mouse tissue panel by RT-PCR and normalized to *Gapdh* expression. B, *Hnf1a* (black bars) *and Hnf1β* (white bars) mRNA levels were measured in a mouse tissue panel by RT-PCR and normalized to *Gapdh* expression. Data represents three independent experiments ± SD. * $P < .05$. Human kidney tissues were co-stained for PCBD2 (green), (C) NCC (red), (D) UMOD (red), (E) AQP2 (red). Scale bar represents 20 μm.

of PCBD2 in the kidney, immunohistochemical analysis of healthy human kidney tissue was performed. PCBD2 staining was most abundant in the outer medulla and co-localized with uromodulin (UMOD), a marker for the thick ascending loop of Henle (TAL) (Figure 3C). In addition, PCBD2 co-localized with Na^+/Cl^- cotransporter (NCC) in the DCT (Figure 3D). We detected no expression of PCBD2 in the CD, using Aquaporin 2 (AQP2) as a marker (Figure 3E).

3.4 | PCBD2 mediates HNF1β promoter activation different from PCBD1

To examine whether PCBD2 regulates the transcriptional activity of HNF1β, a dual luciferase promoter assay was performed. HEK293 cells were co-transfected with luciferase constructs, containing the promoter of *FXYD2* or *KCNJ16*, which are known transcriptional targets of HNF1β in the kidney.[4,5] Promoter activation of Na^+/K^+

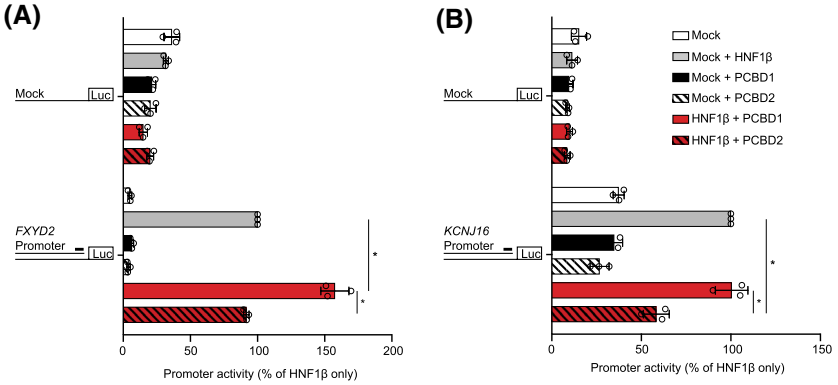

FIGURE 4 HNF1β-mediated gene transcription is differently regulated by PCBD1 and PCBD2. A, HEK293 cells were transiently transfected with a luciferase construct carrying the human *FXYD2* promoter, or a mock construct. Promoter activity was tested in presence or absence of HNF1βand with or without the presence of PCBD1 and PCBD2. B, HEK293 cells were transiently transfected with a luciferase construct carrying the human *KCNJ16* promoter, or a mock construct. Promoter activity was tested in presence or absence of HNF1β and with or without the presence of PCBD1 and PCBD2. Data represents three independent experiments ± SD. * $P < .05$

ATPase subunit gamma (*FXYD2*) was increased by 52% in the presence of co-factor PCBD1, while PCBD2 did not enhance promoter activation by HNF1β (Figure 4A). Promoter activation of *KCNJ16*, encoding the inwardly rectifying K^+ channel 5.1, did not increase in presence of PCBD1 (Figure 4B). In contrast, PCBD2 significantly decreased HNF1β-mediated promoter activation of *KCNJ16* by 42% (Figure 4B).

3.5 | "Kinetic hotspot" does not explain distinct co-factor activities of PCBD1 and PCBD2

The amino acid sequences of both mouse and human PCBD1 and PCBD2 share 48% identity and have a similarity of 88% within the recognition helix (Figure S2A). The recognition helices of PCBD1 and PCBD2, responsible for HNF1 binding and homotetramerization, differ at three residues: 45R-72Q, 51T-78S, and 61D-88N (Figure 5A,C). The major difference is located at the center of the recognition helix at residues 51 and 78 of PCBD1 and PCBD2, respectively (Figure 5A,C). The serine residue in PCBD2, corresponding to T51 in PCBD1, allows a water molecule to be present within the homotetramer.[28] This change results in low stability of the PCBD2 tetramer and, therefore, preferred association with HNF1α molecules.[28,29] The bulkier T51 residue of PCBD1 prevents a water molecule from binding, establishing a hyper stable tetrameric complex that does not form complexes with HNF1 in solution but requires co-folding of the two proteins.[10,30,31] We hypothesized that this "kinetic hotspot" could affect the HNF1β activation properties of PCBD1 and PCBD2 (Figure 5A). To this end, constructs were generated expressing mutant PCBD1-T51S and the corresponding PCBD2-S78T mutant. Again, HEK293 cells were co-transfected with luciferase constructs, containing the *FXYD2* promoter, with or without overexpression of HNF1β and PCBD1, PCBD2, PCBD1-T51S, or PCBD2-S78T. HNF1β-mediated promoter activation of *FXYD2* was not changed in presence of co-factor PCBD1 compared to PCBD1-T51S (Figure 5B). Similarly, the serine to threonine mutation in PCBD2 did not affect promoter activation by HNF1β compared to WT PCBD2 (Figure 5B).

3.6 | N-terminal sequence of PCBD2 is required for its co-factor function

The PCBD2 amino acid sequence contains an additional 27 amino acids in the NH_2 (N)-terminus that are not present in the PCBD1 sequence (Figure 5C). Using the PSIPRED server we could predict that part of this N-terminal strand likely forms an extra alpha helix (Figure 5C).[32] We hypothesized that the N-terminal sequence of PCBD2 might explain the differential activities of PCBD1 and PCBD2 regarding HNF1β co-activation. Therefore, constructs of PCBD2 were generated lacking the N-terminal amino acids from 1 to 27 and luciferase assays were performed. Interestingly, *FXYD2* promoter activity mediated by HNF1β was significantly enhanced in the presence of PCBD2 lacking the 27 N-terminal amino acid sequence compared to WT PCBD2 (Figure 5D).

4 | DISCUSSION

In the present study PCBD2 was identified as a novel interaction partner of HNF1β. PCBD2 modulates HNF1β promoter activation of genes involved in electrolyte homeostasis, different from PCBD1. Specifically, PCBD2 decreased promoter activity of *KCNJ16* while PCBD1 did not alter HNF1β-mediated promoter activation. The *FXYD2* promoter showed increased activity in presence of PCBD1 while

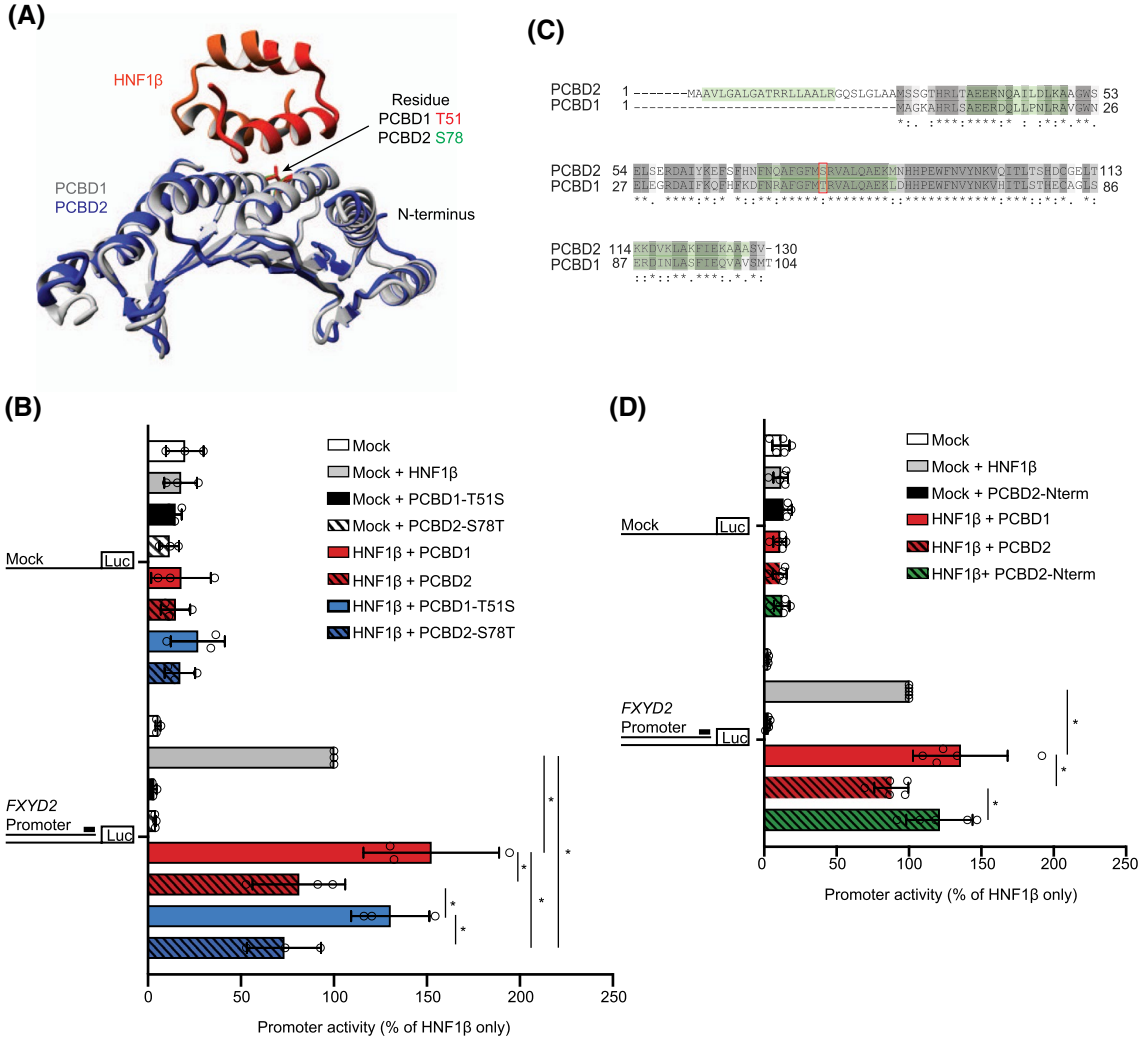

FIGURE 5 N-terminal sequence of PCBD2 is required for its co-factor function. A, Homology model of the PCBD1/2-HNF1β dimerization domain tetramer modeled using the structures of the PCBD1-HNF1α dimerization domain (HNF1α-D) complex (Protein Data Bank ID code 1F93) and the structure of PCBD2 (Protein Data Bank ID code 4C45). PCBD1 (gray), PCBD2 (blue), and HNF1β dimerization domain dimer (red/orange). The side chain of residues T51 and S78 are shown in green and red, respectively. B, HEK293 cells were transiently transfected with a luciferase construct carrying the human *FXYD2* promoter, or a mock construct. Promoter activity was tested in presence or absence of HNF1β and with or without the presence of PCBD1, PCBD2, PCBD1-T51S, or PCBD2-S78T. Data represents three independent experiments ± SD. * $P < .05$. C, Amino acid sequences of human PCBD1 and PCBD2 were aligned using the align tool of Uniprot. Green: Alpha helices, predicted by the PSIPRED server for PCBD2, Gray: Degree of sequence similarity, Red box: "kinetic hotspot." D, HEK293 cells were transiently transfected with a luciferase construct carrying the human *FXYD2* promoter, or a mock construct. Promoter activity was tested in presence or absence of HNF1β and with or without the presence of PCBD1, PCBD2, PCBD2 lacking the N-terminus. Data represents five independent experiments ± SD. * $P < .05$

PCBD2 did not affect *FXYD2* promoter activity. Further studies should confirm whether the unique effects of PCBD1 and PCBD2 on HNF1β activity can be extended to additional HNF1β-target genes involved in cystogenesis, kidney development or intestinal function.

PCBD2 is classified as a moonlighting protein, as it participates in two unrelated biological processes. In the cytosol PCBD2 mediates recycling of tetrahydrobiopterin, which is a co-factor for amino acid hydroxylases. Next to its enzymatic function PCBD2 has been described as a dimerization co-factor of HNF1α, however an interaction with HNF1β has not been reported before.[28] The protein is homologous to PCBD1, in which mutations have previously been demonstrated to cause hyperphenylalaninemia, hypomagnesemia, and diabetes.[28,33,34] Indeed, the interaction of PCBD1 with HNF1β was confirmed in our studies.[10,15,27] Furthermore, multiple CD-specific genes were recognized in the pull-downs as well as genes known to be characteristic for other kidney segments including HNF1α and KIM-1 that are thought to be expressed by the proximal tubule (PT) only.[35-37] Interestingly, in contrast to the NE pull-down we did not identify HNF1α among significant and nonsignificant interactors in the NPE pull-down. This finding indicates that PCBD2, like PCBD1, directly binds to HNF1β independently of HNF1α. However,

in both the NE and the NPE pull-down PCBD2 was found less frequently in complex with HNF1β compared to PCBD1. Remarkably, other studies using human fetal kidney and adult mouse kidney cells, identified additional HNF1β interaction partners including E4F1,[38] TRM26,[38] and Zyxin.[39] The differences between these studies indicate that distinct co-factors may interact with HNF1β depending on the renal cell type and stage of kidney development.

Despite their significant homology, our luciferase experiments demonstrate that PCBD1 and PCBD2 have different effects on HNF1β-induced transcriptional activity. In presence of PCBD1, HNF1β-mediated promoter activation of *FXYD2* was increased (52%), whereas it was unaltered by PCBD2. Additionally, we have performed HNF1β promoter luciferase assays with the *KCNJ16* promoter in presence of PCBD1 for the first time. Surprisingly, PCBD1 did not increase the HNF1β-induced promoter activation of *KCNJ16* as it does for the *FXYD2* promoter. The *KCNJ16* promoter activation was reduced (42%) in presence of PCBD2 while PCBD1 did not alter HNF1β function. The major difference in the recognition helices of PCBD1 and PCBD2 is located at residue 51 and 78, respectively.[28,29,40] However, mutating this "kinetic hotspot" did not modulate their transcriptional activity. In contrast, deleting the N-terminal sequence of PCBD2, that is missing in the PCBD1 sequence, did increase HNF1β promoter activity compared to the activity observed in presence of the normal functioning PCBD2. The position of this alpha helix in the PCBD2 protein structure is presently unknown. Nevertheless, it could be hypothesized that this helix directly interacts with HNF1β or is essential for the recruitment of additional regulatory proteins.

Indeed, the saddle shaped surface of PCBDs is optimal for protein-protein binding. Previous studies demonstrated that mutagenesis of residues lining this concave shaped surface in PCBD1 decreased transcriptional activity of HNF1α.[41] Moreover, interactions with the co-factors may be specific for a PCBD isoform. For instance, Sirtuin 1 (SIRT1) deacetylates two lysine residues of PCBD2 (K124 and K131) that are not conserved in the PCBD1 sequence.[42] Intestine-specific knock out of Sirt1 in mice led to decreased transcriptional activation of HNF1α/β-target gene Farnesoid X receptor (*Fxr)*, likely through hyperacetylation of PCBD2.[42,43] This modification might stabilize the homotetrameric form of PCBD2, thereby decreasing the formation of PCBD2-HNF1α complexes.[42] Our interaction assay did not identify additional co-factors of transcriptional activity, which may suggest that these interactions are transient.

As a consequence of the bifunctional role of PCBD1 and PCBD2 their localization is nuclear as well as cytoplasmic. We show that the nuclear localization of both PCBD1 and PCBD2 significantly increases in presence of HNF1β at the expense of the cytoplasmic localization. Interestingly, in our western blot analysis, the PCBD molecules were detected at a size ranging from 17 kDa to approximately 12 kDa, suggesting that these proteins are posttranslationally modified both in the cytoplasmic and nuclear fractions. Notably, PCBD molecules in the immunoprecipitation fractions demonstrated a narrower size distribution compared to the input fraction, indicating that only a subset of the modified PCBD molecules interact with HNF1β. These observations should be interpreted with caution as we did not exclude the possibility that these distinctly sized proteins are degradation products of the co-factors. Nevertheless, the role of posttranslational modifications for the PCBD-HNF1β interaction would be interesting subjects for future studies.

The distinct transcriptional activities of PCBD1 and PCBD2 provide a mechanism to differentially regulate HNF1β function. Indeed, our expression analysis demonstrated that Pcbd1 and Pcbd2 expression is specific for different tissues. Whereas *Pcbd1* predominantly is expressed in kidney and liver, *Pcbd2* was also highly expressed in lung, spleen, and fat tissue. Within the kidney, immunohistochemical analysis showed enrichment of the PCBD2 staining in the TAL and DCT, while a study from Ferrè et al[15] reported PCBD1 protein expression primarily in the DCT. In contrast, transcriptomics data of rat and human kidney show mRNA expression of *Pcbd1* in all renal tubules.[37,44] Accordingly, proteomics data in rat reported expression of PCBD1 and PCBD2 in all epithelial cells of the kidney except the cells of the glomeruli.[35] In contrast to our immunohistochemistry analysis, the expression of the PCBD molecules in PT cells was one of the highest.[35] Although the data discussed here vary from human and mouse to rat, it is likely PCBD1 expression is not restricted to the DCT as observed by Ferrè et al.[15] Interesting to note is that most datasets described a 2- to 10-fold higher expression of PCBD1 in renal tubules compared to PCBD2.[35]

Transcriptional targets of HNF1β in the TAL involved in electrolyte transport and cystogenesis are calcium-sensing receptor *(CASR), PKHD1* and *KCNJ16*.[4,6,45] In the DCT, *FXYD*2 and *KCNJ16* are the main transcriptional targets. Interestingly, while both PCBD2 and PCBD1 are expressed in the DCT, our luciferase experiments show that PCBD1 enhances the activation of the *FXYD2* promoter by HNF1β while PCBD2 does not.[15] These different transcriptional activities of the PCBD molecules might explain why PCBD2 cannot compensate for loss of PCBD1 function in patients with PCBD1 mutations. HNF1β is known to regulate many more genes involved in kidney function and development besides ion transport in the DCT and TAL. The function of PCBD1 and PCBD2 in HNF1β-mediated gene transcription could, therefore, be different for genes involved in cystogenesis, kidney development or intestinal function.

Interestingly, in our mouse tissue panel *Pcbd1* and *Pcbd2* are expressed in spleen and fat while these tissues neither express *Hnf1a* or *Hnf1b* nor display PAH activity. Previous

studies in Xenopus showed that PCBD1 is expressed earlier in vertebrate development than HNF1α and PAH.[46] It was also found in skin, brain, and pigmented epithelium where no Hnf1a or Hnf1b expression was detected.[46] In line with our findings this suggests an unknown function of PCBD1 and PCBD2 in these tissues, presumably binding to other transcription factor besides HNF1α and HNF1β regulating their function.[46,47]

Our results showing that *PCBD2* is a novel distinct regulator of HNF1β activity, opens up new perspectives to study the heterogenic and complex HNF1β function. *PCBD2* has been associated with tumor growth, type two diabetes, and osteoporosis.[48-51] Indeed, two GWAS studies identified risk variants in the *PCBD2* gene, rs299371-T, and rs319598-C, that are associated with whole bone mineral density and type two diabetes susceptibility.[49,50] Given the central role of HNF1β in kidney development, magnesium homeostasis, and diabetes, the PCBD2-HNF1β interaction may explain these associations.

In conclusion, our results provide an example of gene regulation by transcription factors mediated by different expression patterns and activities of co-factors. Specifically, we demonstrate that despite the high similarity in function and sequence of PCBD1 and PCBD2, the two co-factors are capable of modulating HNF1β transcriptional activity in a different fashion.

ACKNOWLEDGMENTS

The authors thank Devin Verbueken for his excellent technical support. This work was financially supported by grants from the Dutch Kidney Foundation (Large Kolff grant 17OKG07) and the Netherlands Organization for Scientific Research (NWO Veni 016.186.012, Vici 016.130.668). The Vermeulen lab is part of the Oncode Institute, which is partly funded by the Dutch Cancer Society.

CONFLICT OF INTEREST

The authors have no financial conflicts of interest.

AUTHOR CONTRIBUTIONS

L.E. Tholen, J.G.J. Hoenderop, M. Vermeulen, and J.H.F. de Baaij designed the research studies; L.E. Tholen and P.W.T.C. Jansen conducted the mass spectrometry experiments and analyzed the data; L.E. Tholen and C. Bos conducted all other experiments and/or analyzed the data, H. Venselaar performed the homology modeling of the HNF1β interaction domain, and L.E. Tholen, J.G.J. Hoenderop, and J.H.F. de Baaij wrote the manuscript. All authors corrected the manuscript and approved the final version.

ORCID

Lotte E. Tholen https://orcid.org/0000-0003-2838-8636
Caro Bos https://orcid.org/0000-0001-5016-9435
Pascal W. T. C. Jansen https://orcid.org/0000-0003-3064-5742
Hanka Venselaar https://orcid.org/0000-0001-9824-6559
Michiel Vermeulen https://orcid.org/0000-0003-0836-6894
Joost G. J. Hoenderop https://orcid.org/0000-0002-1816-8544
Jeroen H. F. de Baaij https://orcid.org/0000-0003-2372-8486

REFERENCES

1. Coffinier C, Barra J, Babinet C, Yaniv M. Expression of the vHNF1/HNF1b homeoprotein gene during mouse organogenesis. *Mech Dev*. 1999;89:211-213.
2. Verhave JC, Bech AP, Wetzels JFM, Nijenhuis T. Hepatocyte nuclear factor 1 -associated kidney disease: more than renal cysts and diabetes. *J Am Soc Nephrol*. 2016;27(2):345-353.
3. Adalat S, Woolf AS, Johnstone KA, et al. HNF1B mutations associate with hypomagnesemia and renal magnesium wasting. *J Am Soc Nephrol*. 2009;20:1123-1131.
4. Kompatscher A, de Baaij JHF, Aboudehen K, et al. Loss of transcriptional activation of the potassium channel Kir5.1 by HNF1β drives autosomal dominant tubulointerstitial kidney disease. *Kidney Int*. 2017;92(5):1145-1156.
5. Ferrè S, Veenstra GJC, Bouwmeester R, Hoenderop JGJ, Bindels RJM. HNF-1B specifically regulates the transcription of the ca-subunit of the Na+/K+-ATPase. *Biochem Biophys Res Commun*. 2011;404:284-290.
6. Hiesberger T, Bai Y, Shao X, et al. Mutation of hepatocyte nuclear factor-1β inhibits Pkhd1 gene expression and produces renal cysts in mice. *J Clin Invest*. 2004;113(6):814-825.
7. Verdeguer F, Le Corre S, Fischer E, et al. A mitotic transcriptional switch in polycystic kidney disease. *Nat Med*. 2010;16(1):106-110.
8. Barbacci E, Chalkiadaki A, Masdeu C, et al. HNF1b/TCF2 mutations impair transactivation potential through altered co-regulator recruitment. *Hum Mol Genet*. 2004;13(24):3139-3149.
9. Soutoglou E, Viollet B, Vaxillaire M, Yaniv M, Pontoglio M, Talianidis I. Transcription factor dependent regulation of CBP and P/CAF histone acetyltransferase activity. *EMBO J*. 2001;20(8):1984-1992.
10. Mendel DB, Khavari PA, Conley PB, et al. Characterization of a cofactor that regulates dimerization a mammalian homeodomain protein. *Science*. 2004;254:1762-1768.
11. Huberts DHEW, Van Der KIJ. Moonlighting proteins: an intriguing mode of multitasking. *Biochim Biophys Acta*. 2010;1803:520-525.
12. Citron BA, Davis MD, Milstien S, et al. Identity of 4a-carbinolamine dehydratase, a component of the phenylalanine hydroxylation system, and DCoH, a transregulator of homeodomain proteins. *Proc Natl Acad Sci USA*. 1992;89:11891-11894.
13. Werner ER, Blau N, Thöny B. Tetrahydrobiopterin: biochemistry and pathophysiology. *Biochem J*. 2011;414:397-414.
14. Simaite D, Kofent J, Gong M, et al. Recessive mutations in PCBD1 cause a new type of early-onset diabetes. *Diabetes*. 2014;63:3557-3564.
15. Ferrè S, de Baaij JHF, Ferreira P, et al. Mutations in PCBD1 cause hypomagnesemia and renal magnesium wasting. *J Am Soc Nephrol*. 2014;25(3):574-586.
16. Desgrange A, Heliot C, Skovorodkin I, et al. HNF1B controls epithelial organization and cell polarity during ureteric bud

branching and collecting duct morphogenesis. *Development*. 2017;144:4704-4719.

17. Lokmane L, Heliot C, Garcia-villalba P, Fabre M, Cereghini S. vHNF1 functions in distinct regulatory circuits to control ureteric bud branching and early nephrogenesis. *Development*. 2010;137:347-357.
18. Dignamr JD, Lebovitz RM, Roeder RG. Accurate transcription initiation by RNA polymerase II in a soluble extract from isolated mammalian nuclei. *Nucleic Acids Res*. 1983;1(5):1475-1489.
19. Hubner NC, Mann M. Extracting gene function from protein—protein interactions using Quantitative BAC InteraCtomics (QUBIC). *Methods*. 2011;53(4):453-459.
20. Rappsilber J, Mann M, Ishihama Y. Protocol for micro-purification, enrichment, pre-fractionation and storage of peptides for proteomics using StageTips. *Nat Protoc*. 2007;2(8):1896-1906.
21. Cox J, Mann M. MaxQuant enables high peptide identification rates, individualized p.p.b.-range mass accuracies and proteome-wide protein quantificatio. *Nat Biotechnol*. 2008;26(12):1367-1372.
22. Tyanova S, Temu T, Sinitcyn P, et al. The Perseus computational platform for comprehensive analysis of (prote)omics data. *Nat Methods*. 2016;13(9):731-7340.
23. Smits AH, Jansen PWTC, Poser I, Hyman AA, Vermeulen M. Stoichiometry of chromatin-associated protein complexes revealed by label-free quantitative mass spectrometry-based proteomics. *Nucleic Acids Res*. 2013;41(1):1-8.
24. Krieger E, Koraimann G, Vriend G. Increasing the precision of comparative models with YASARA NOVA—a self-parameterizing force field. *PROTEINS Struct Funct Genet*. 2002;402(47):393-402.
25. Vriend G. WHAT IF: a molecular modeling and drug design program. *J Mol Graph*. 1990;8(3):52-56.
26. Meyer AH, Blatow M, Rozov A, Monyer H. In vivo labeling of parvalbumin-positive interneurons and analysis of electrical coupling in identified neurons. *J Neurosci*. 2002;22(16):7055-7064.
27. Mendel DB, Hansen LP, Graves MK, Conley B, Crabtree GR. HNF-1a and HNF-1b (vHNF-1) share dimerization and homeo domains, but not activation domains, and form heterodimers in vitro. *Genes Dev*. 1991;5:1042-1056.
28. Rose RB, Pullen KE, Bayle JH, Crabtree GR, Alber T. Biochemical and structural basis for partially redundant enzymatic and transcriptional functions of DCoH and DCoH2. *Biochemistry*. 2004;43:7345-7355.
29. Rho H, Jones CN, Rose RB. Kinetic stability may determine the interaction dynamics of the bifunctional protein DCoH1, the dimerization cofactor of the transcription factor HNF-1a. *Biochemistry*. 2010;49:10187-10197.
30. Rose RB, Bayle JH, Endrizzi JA, Cronk JD, Crabtree GR, Alber T. Structural basis of dimerization, coactivator recognition and MODY3 mutations in HNF-1α. *Nat Struct Biol*. 2000;7(9):744-748.
31. Ficner R, Sauer UH, Stier G, Suck D. Three-dimensional structure of the bifunctional protein PCD/DCoH, a cytoplasmic enzyme interacting with transcription factor HNF1. *EMBO J*. 1995;14(9):2034-2042.
32. Buchan DWA, Jones DT. The PSIPRED protein analysis workbench: 20 years on. *Nucleic Acids Res*. 2019;47(W1):W402-W407.
33. Citron BA, Kaufman S, Milstien S, Naylor EW, Greene CL, Davis MD. Mutation in the 4a-carbinolamine dehydratase gene leads to mild hyperphenylalaninemia with defective cofactor. *Metabolism*. 1993;S3:768-774.
34. Thöny B, Neuheiser F, Kierat L, et al. Hyperphenylalaninemia with high levels of 7-biopterin is associated with mutations in the PCBD gene encoding the bifunctional protein pterin-4a- carbinolamine dehydratase and transcriptional coactivator (DCoH). *Am J Hum Genet*. 1998;62:1302-1311.
35. Limbutara K, Chou C, Knepper MA. Quantitative proteomics of all 14 renal tubule segments in rat. *J Am Soc Nephrol*. 2020;31(6):1255-1266.
36. Adam M, Potter AS, Potter SS. Psychrophilic proteases dramatically reduce single-cell RNA-seq artifacts: a molecular atlas of kidney development. *Development*. 2017;114:3625-3632.
37. Muto Y, Wilson PC, Wu H, Waikar SS, Humphreys BD. Single cell transcriptional and chromatin accessibility profiling redefine cellular heterogeneity in the adult human kidney. *bioRxiv*. 2020. https://doi.org/10.1101/2020.06.14.151167
38. Dudziak K, Mottalebi N, Senkel S, et al. Transcription factor HNF1 b and novel partners affect nephrogenesis. *Kidney Int*. 2008;74(2):210-217.
39. Choi Y, Mcnally BT, Igarashi P. Zyxin regulates migration of renal epithelial cells through activation of hepatocyte nuclear factor-1b. *Am J Ren Physiol*. 2013;305(1):100-110.
40. Wang D, Coco MW, Rose RB. Interactions with the bifunctional interface of the transcriptional coactivator DCoH1 are kinetically regulated. *J Biol Chem*. 2015;290(7):4319-4329.
41. Johnen G, Kaufman S. Studies on the enzymatic and transcriptional activity of the dimerization cofactor for hepatocyte nuclear factor 1. *Proc Natl Acad Sci USA*. 1997;94:13469-13474.
42. Kazgan N, Metukuri MR, Purushotham A, et al. Intestine-specific deletion of Sirt1 in mice impairs DCoH2– HNF1α–FXR signaling and alters systemic bile acid homeostasis. *Gastroenterology*. 2015;146(4):1006-1016.
43. Aboudehen K, Noureddine L, Cobo-Stark P, et al. Hepatocyte nuclear factor–1 β regulates urinary concentration and response to hypertonicity. *J Am Soc Nephrol*. 2017;28(10):2887-2900.
44. Lee JW, Chou C, Knepper MA. Deep sequencing in microdissected renal tubules identifies nephron segment—specific transcriptomes. *J Am Soc Nephrol*. 2015;26(11):2669-2677.
45. Kompatscher A, De BJHF, Aboudehen K, et al. Transcription factor HNF1B regulates expression of the calcium-sensing receptor in the thick ascending limb of the kidney. *Am J Ren Physiol*. 2018;315:F27-F35.
46. Pogge E, Ryffel GU. Developmental expression of the maternal protein XDCoH, the dimerization cofactor of the homeoprotein LFB1 (HNF1). *Development*. 1995;121:1217-1226.
47. Pogge E, Senkel S, Ryffel GU. Ectopic pigmentation in Xenopus in response to DCoH/PCD, the cofactor of HNF1 transcription factor/pterin-4acarbinolamine dehydratase. *Mech Dev*. 2000;91:53-60.
48. Zhang D, Yang N. MiR-3174 functions as an oncogene in rectal cancer by targeting PCBD2. *Eur Rev Med Pharmacalogical Sci*. 2019;23:2417-2426.
49. Morris JA, Kemp JP, Youlten SE, et al. An atlas of genetic influences on osteoporosis in humans and mice. *Nat Genet*. 2019;51(2):258-266.
50. DIAbetes Genetics Replication and Meta-analysis (DIAGRAM) Consortium, Asian Genetic Epidemiology Network Type 2 Diabetes (AGEN-T2D) Consortium, South Asian Type 2 Diabetes (SAT2D), Mexican American Type 2 Diabetes (MAT2D) Type 2 Diabetes Genetic Explorati T 2 DGE by N Sequencing in Multi-ES (T2D-GC). Genome-wide trans-ancestry meta-analysis provides

insight into the genetic architecture of type 2 diabetes susceptibility. *Nat Genet*. 2014;46(3):234-244.
51. Bueno R, De Rienzo A, Dong L, et al. Second generation sequencing of the mesothelioma tumor genome. *PLoS One*. 2010;5(5):e10612.

SUPPORTING INFORMATION

Additional Supporting Information may be found online in the Supporting Information section.

How to cite this article: Tholen LE, Bos C, Jansen PWTC, et al. Bifunctional protein PCBD2 operates as co-factor for hepatocyte nuclear factor 1β and modulates gene transcription. *The FASEB Journal*. 2021;35:e21366. https://doi.org/10.1096/fj.202002022R